Controls on permafrost-related landform distributions, Dempster and Inuvik-Tuktoyaktuk Highway corridors, northwestern Canada

Peter D. Morse[1], Wendy E. Sladen[1], Ryan J.H. Parker[1], Sharon L. Smith[1] & Steven V. Kokelj[2]

[1]*Geological Survey of Canada, Natural Resources Canada, Ottawa, Ontario, Canada*

[2]*Northwest Territories Geological Survey, Government of Northwest Territories, Yellowknife, Northwest Territories, Canada*

Abstract

Knowledge of the distributions of permafrost landforms are important because they serve as indicators of ground ice conditions and thaw sensitivity. Permafrost degradation at these locations changes the physiographic, hydrologic, and ecologic conditions and impacts northern landscapes, wildlife, and infrastructure. Geospatial inventories of these landforms are time-consuming to make and are often limited in extent and landform type, reducing their utility to support informed decisions regarding land management, resource development, infrastructure design and maintenance, and climate adaptation strategies. Such inventories did not exist in northwestern Canada where permafrost degradation is modifying environmental system dynamics and challenging the performance of the Dempster and Inuvik-Tuktoyaktuk Highway (DH-ITH). We analyzed a new, comprehensive geodatabase of 8746 permafrost-related landforms (periglacial, mass movement, and hydrological features) developed for an 875 km-long, 10 km-wide DH-ITH corridor. Though intuitive, our findings demonstrate how broad-scale spatial distributions of 25 different permafrost-related landforms relate to surficial geology, glacial history, and permafrost conditions, which are intrinsic to the set of physiographic regions in this area.

1 Introduction

In northwestern Canada (Figure 1), a range of physiographic settings exist as a function of variations in geology (Roots and Hart 2004), Quaternary deposits and history (Thomas and Rampton 1982a,b,c,d,e,f; Rampton 1988; Duk-Rodkin and Hughes 1992a,b; Gordey and Makepeace 2003), and permafrost conditions (Heginbottom et al. 1995). These physiographic variations have been characterized into distinct regions (Matthews 1986; Rampton 1988; Bostock 2014), and since the Second World War there has been great effort to study the processes and landforms that define them (e.g., Mackay 1963). This history of research has supported development of infrastructure for transportation, communities, and natural resource exploration and continues to this day (e.g., Kokelj et al. 2021). However, there are still great uncertainties regarding the distribution of ground ice, and consequently thaw sensitive terrains, despite recent, significant advancements on modelling regional ground ice distribution (e.g., O'Neill et al. 2019; Castagner et al. 2023).

Many permafrost-related landforms indicate ground ice presence and thaw susceptibility. Knowledge of their distributions is important, because permafrost degradation at these locations reduces ground stability, modifies terrain, and reconfigures drainage patterns, affecting terrestrial and aquatic ecosystems (e.g., Kokelj and Jorgenson 2013), and challenges the integrity of northern infrastructure (Hjort et al. 2022). Geospatial inventories of permafrost-related landforms can facilitate understanding of the broad-scale controls on their distributions and their associations with terrain settings (i.e., physiography, surficial geology, glacial history, and permafrost and ground ice conditions).

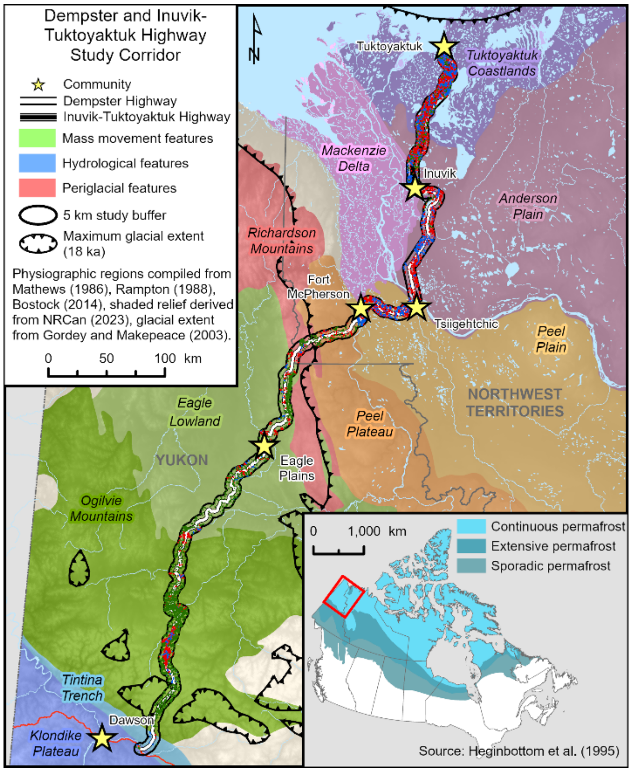

Figure 1. The DH-ITH mapping corridor, feature class distributions, physiographic regions, and maximum glacial extent. Inset shows study area location and continuous and discontinuous permafrost extents.

https://doi.org/10.52381/ICOP2024.140.1

Empirically based datasets are required to provide testing and validation data for predictive mapping activities (e.g., Rudy et al. 2019), and these data are also needed to increase the quality and quantity of information for decision-making related to land management, resource development, infrastructure design and maintenance, and climate change adaptation strategies (e.g., McKillop et al. 2016; Weiss et al. 2021).

Such inventories are typically limited to small extents, few landform types, or to broad scales using approaches that do not map individual landforms (e.g., Charbonneau et al. 2018; Gibson et al. 2021; Kokelj et al. 2021; Lou et al. 2022; Wolfe et al. 2023). Consequently, few detailed inventories are broad in spatial extent and comprehensive in the potential suite of thaw susceptible landforms, and until this study no comprehensive inventory has been developed for northwestern Canada.

The combined Dempster Highway and Inuvik-Tuktoyaktuk Highway (DH-ITH) corridor region (Figure 1) is an ideal regional north-south transect to develop a comprehensive inventory and investigate broad-scale controls on permafrost-related landform distributions, including surficial geology, glacial history, permafrost extent and ice content, and physiographic region. Changing permafrost conditions are significantly impacting transportation infrastructure at various locations along this corridor (Stockton et al. 2021), with new transmission infrastructure currently being buried adjacent to the DH. Thus, a multivariable landform inventory could be used to determine variation in the terrain sensitivity and potential vulnerabilities of the infrastructure to inform adaptation strategies and maintenance planning.

The 875 km-long, all-season, gravel DH-ITH connects southern Canada to the Arctic Ocean (Figure 1). Completed in 1978, the DH starts within unglaciated terrain of the Klondike Plateau in Yukon near Dawson (64.1°N), crosses the Tintina Trench, and runs northward through the high-relief Ogilvie Mountains of the Northern Cordillera. It continues through the rolling, unglaciated Eagle Lowland (or Plain) and then up into the higher relief of the unglaciated southern ranges of the Richardson Mountains where it crosses the Yukon – Northwest Territories border at Wright Pass (67.0°N). It then traverses the ice-rich morainal Peel Plateau and descends through the comparatively subdued relief of the Peel Plain with hummocky rolling moraine and poorly drained till plain with fens and peatlands until it meets the Mackenzie River near Tsiigehtchic. From the north shore of the river, the DH crosses gently-sloping, rolling terrain of Anderson Plain with till veneer and organic deposits, and terminates at Inuvik (68.4°N). Completed in 2017, the ITH begins at Inuvik and runs northward across the Anderson Plain where there is a range of unconsolidated deposits (the study corridor here includes Mackenzie Delta alluvium). At treeline, the route transitions to the Tuktoyaktuk Coastlands characterized by rolling and hummocky tills with dispersed lacustrine plains, reaching the Beaufort Sea coast at Tuktoyaktuk (69.4°N). Permafrost within the corridor is continuous except for the most southern ~100 km that is in extensive discontinuous permafrost (Heginbottom et al. 1995), and various forms of ground ice are present, dominated by wedge ice, segregated ice, intrusive ice, and buried glacial ice (Burn et al. 2015; O'Neill et al. 2019).

In this context, our aim is to provide an (qualitative) assessment of factors that influence the distribution of permafrost-related landforms and terrain sensitivity along the DH-ITH corridor. Our objectives are to: i) use a comprehensive approach to identify and map thermokarst and periglacial landforms, and ii) summarize the distributions of permafrost-related landforms based on permafrost and ground ice conditions, surficial geology, glacial history, and physiographic region (Figures 1, 2 and 3). To do this we analyze a geodatabase of permafrost-related landforms mapped within a 10 km-wide corridor (8560 km^2) that extends to the "height of the land" and is centred on the combined DH-ITH alignment (Sladen et al. 2022).

2 METHODOLOGY

The geodatabase of permafrost-related landforms for the DH-ITH corridor (Sladen et al. 2022) was generated using a new methodological protocol co-developed by the Geological Survey of Canada and the Northwest Territories Geological Survey to classify and digitize geomorphic features of permafrost terrain using high-resolution (0.6 m) satellite imagery (Sladen et al. 2021). Landforms were identified at 1:10,000 scale based on Canadian Digital Elevation Model (CDEM; NRCan 2023), and digitized at 1:5000 scale in a 3-D environment using Summit Evolution^{TM} and ArcMAP^{TM} platforms. Landforms were classified according to main formational process yielding sets of periglacial, mass movement, and hydrological features (Table 1). Landform verification was conducted in the field on a subset of mapped features during summer 2018, and other features were verified using Northwest Territories Ecological Land Classification Photos (NWTCG 2020). Landform attributes were assigned in a geographic information system according to overlay analysis with datasets for physiographic region (Mathews 1986; Rampton 1988; Bostock 2014), surficial geology (Thomas and Rampton 1982a,b,c,d,e,f; Rampton 1988; Duk-Rodkin and Hughes 1992a,b), glacial history (Gordey and Makepeace 2003), and permafrost extent and ground ice conditions (Heginbottom et al. 1995). The spatial data coordinate system used to calculate areas for this analysis is CSRS NAD 1983 datum projected to UTM Zone 8N.

Here we report the spatial density of landforms stratified by: i) continuous high ice (CH), continuous medium-to-high ice (CM-H), continuous low-to-medium ice (CL-M), continuous low ice (CL), and extensive discontinuous low-to-medium ice (EL-M) permafrost units (Heginbottom et al. 1995); ii) alluvium (A), colluvium (C), eolian (E), glaciofluvial (GF), glaciolacustrine (GL), lacustrine (L), moraine/till (M), organic (O), and bedrock (R) surficial geology units (Thomas and Rampton 1982a,b,c,d,e,f; Rampton 1988; Duk-Rodkin and Hughes 1992a,b); iii) glaciated (GLA) and unglaciated (UGLA) glaciation units (Gordey and Makepeace 2003); and iv) Klondike Plateau (KP), Tintina Trench (TT), Ogilvie Mountains (OM), Eagle Lowland (EL), Richardson Mountains (RM), Peel Plateau (PPT), Peel Plain (PPL), Anderson Plain (AP), Mackenzie Delta (MD), and Tuktoyaktuk Coastlands (TC) physiographic regions

(Mathews 1986; Rampton 1988; Bostock 2014). An alternate perspective on presenting landform densities is according to "land" area, but this does not work well for many of the hydrological features, and extensive water bodies (≥ 20% area) are limited to PPL, MD, AP, and TC (Figure 2). Thus, we report densities with respect to total area within the corridor. We do not investigate the roles of elevation or aspect as these local-scale factors of relief are not relevant to all features, and broad-scale influences of relief are captured by the different physiographies that are considered here.

Table 1. Landform classes, codes, counts and areas of based on dominant process and their associated landform types and subtypes.

Landform class	Code	Count (n)	Area (km^2)
Periglacial		5123	300.21
Ice-wedge polygon		3868	190.46
High centre	IWP-H	3204	152.30
Low centre	IWP-L	555	28.90
Undifferentiated	IWP-UN	109	9.26
Palsa	PALSA	4	0.12
Peat plateau complex	PEATP	762	78.07
Pingo	PINGO	113	0.97
String / Net fen	SNF	375	30.65
Unclassified	UN	1	30.65
Mass movement		2435	156.76
Complex	CX	3	0.24
Fall	FA	15	0.80
Flow		2218	152.76
Active-layer detachment	FL-ALD	155	1.76
Debris flow	FL-DF	925	50.96
Rock glacier	FL-RG	40	5.18
Retrogressive thaw slump	FL-RTS	389	4.52
Solifluction	FL-SO	662	87.95
Unclassified	FL-UN	47	2.40
Slide		93	1.17
Rotational slide	SL-RS	5	0.45
Shoreline slump	SL-SS	57	0.28
Unclassified	SL-UN	31	0.44
Unclassified	UN	106	1.80
Hydrological		1188	129.12
Aufeis	AUF	34	1.12
Beaded stream	BS	119	12.29
Drained-lake basin		118	19.74
Fully-drained	DLB-F	27	1.55
Partially-drained	DLB-P	91	18.19
Lake/pond affected by thermokarst	TL	917	95.97

3 Results

With respect to area (Figure 2) and density (Figure 3), nearly 89% of the corridor area is continuous permafrost, with ground ice content generally increasing northward from low and medium at KP and TT to high throughout AP, MD, and TC. The most widespread surficial geology units are C (~39%), M (~32%), and A (~14%). Units C, A, and R (~2% overall), are concentrated in the five southernmost physiographic units that have comparatively high relief (KP northward to RM), with nearly 35% of RM composed of R. Over 95% of these same physiographic regions is outside the maximum limit of the Laurentide Ice Sheet (UGLA). From PPT north to TC, the terrain is entirely GLA, and surficial geology is dominated by glacial deposits M and GF (~6% overall), with the exception of MD physiographic unit with Holocene-age A deposits. In the north, L (~4% overall) is widespread in TC and comprises ~32% of deposits there.

Sladen et al. (2022) inventoried 8746 landforms (~586 km^2) within the DH-ITH corridor, including 5123 periglacial features (~300 km^2), 2435 mass movement features (~157 km^2), and 1188 hydrological features (129 km^2; Figure 1; Table 1). The density of all landforms in the corridor is 6.8%.

According to class, periglacial landforms are the most extensive with respect to area within the corridor (3.5%), followed by mass movement (1.8%), and hydrological (1.5%; Figure 4). Periglacial landforms are present in all physiographic units, with highest densities in TC (15.5%), PPL (12.0%), AP (10.8%), and OM (8.6%), but with densities ≤ 5% in the remaining units. According to permafrost unit, the highest densities of permafrost landforms are in CH (8.0%) and CL-M (4.1%) and are < 1.5% elsewhere. Most periglacial landforms are concentrated in glaciated terrain (5.2% of GLA) and are less dense (2.0%) in UGLA. With respect to surficial geology, nearly 25% of O comprises mappable permafrost landforms, compared to ~13.2%, ~9%, and ~8% for L, GF, and GL respectively, with densities < 5% in remaining units.

Unlike the periglacial class, mass movement and hydrological landforms are strongly partitioned by physiographic unit (Figure 4). Hydrological landform densities range from 0.9 to 9.7% in the four northern most physiographic units but are only 0.0 to 0.2% south of PPL. Hydrological landform densities are nearly zero beyond the maximum glacial limit UGLA, being concentrated in GLA (3.0%). Similarly, hydrological landforms are most dense in CH permafrost (4.5%) and are an order of magnitude less dense in other permafrost units. Hydrological features are most concentrated in A, GF, GL, L, and M surficial geology units with densities ranging from 1.5 to 6.2%, but are nearly absent in other units. Conversely, mass movement landforms are concentrated beyond the extent of the Laurentide ice sheet (3% in UGLA versus 0.5% in GLA), especially in OM (5.5%), EL (1.6%), and RM (1.6%) physiographic units. Mass movement densities are low (0.3%) in CM-H and CH permafrost units but range from 3.4 to 5.6% in other units.

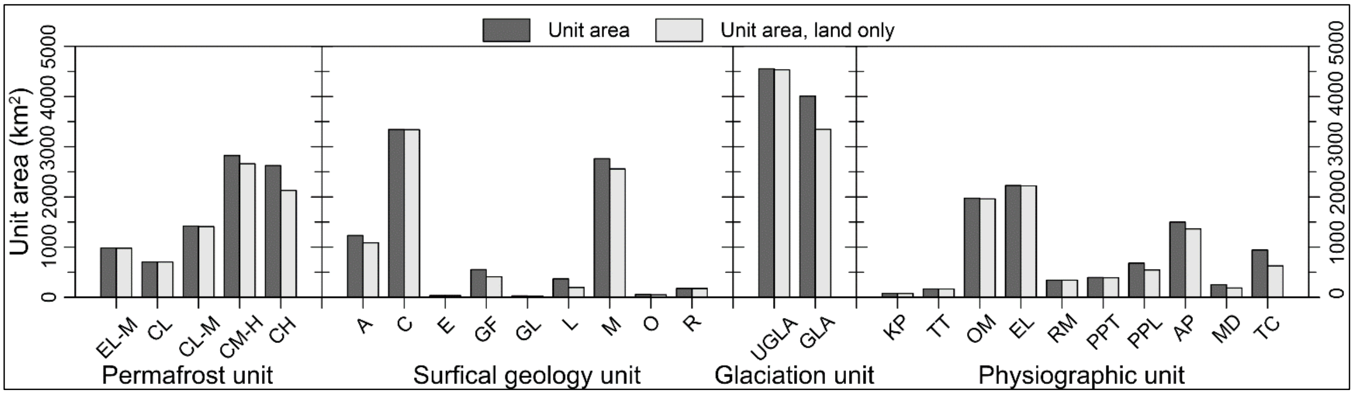

Figure 2. Total area and land-only area (water bodies excluded) with respect to permafrost, surficial geology, glaciation, and physiographic region. Unit codes are as defined in the methodology.

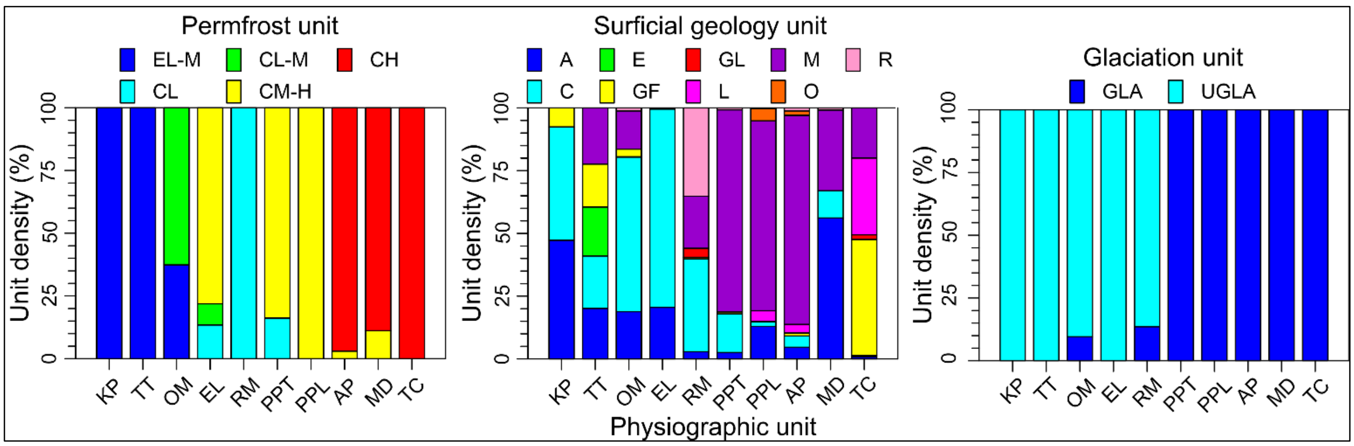

Figure 3. Distributions of permafrost, surficial geology, and glaciation with respect to physiographic region. Unit codes are as defined in the methodology. Physiographic regions are ordered from south to north.

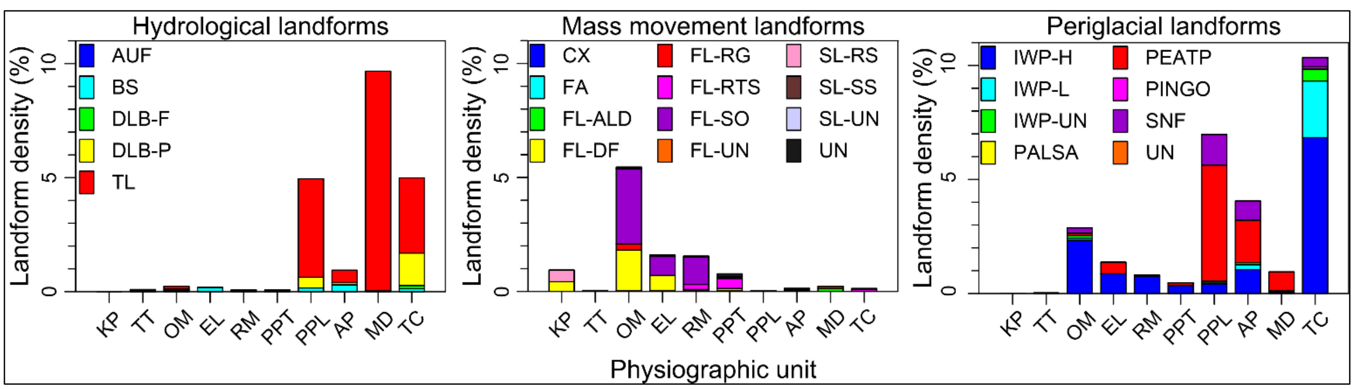

Figure 4. Densities of hydrological, mass movement, and periglacial landform classes with respect to spatial units of permafrost, surficial geology, glaciation, and physiographic region. Unit codes are as defined in the methodology.

With respect to densities of landform type and subtype for each major landform class according to physiographic region (Figure 5), almost 74% of the hydrological landform area comprises TL, and 72% is within PPL (4.3% density), AP (0.5% density), MD (9.6% density), and TC (3.3% density) physiographic units, where another ~14% of hydrological landform area comprises DLB-P in these very same physiographic units. Though densities are ≤ 0.3 everywhere, BS has the third highest contribution to total hydrological landform area (9.5%) and is most dense in AP (0.3%). Areas for AUF and DLB-F hydrological landforms are low (Table 1), with densities generally less than 0.1%.

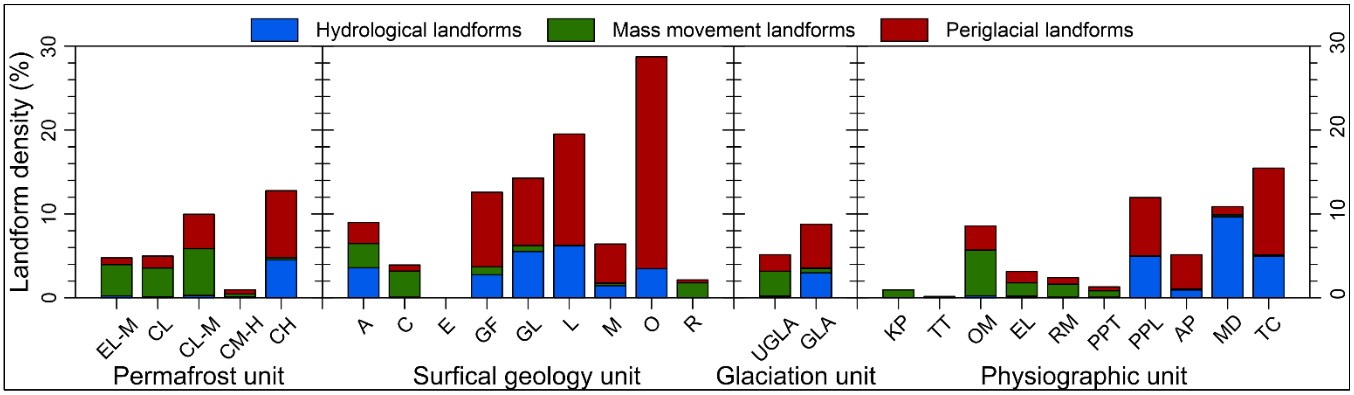

Figure 5. Densities of landforms for hydrological, mass movement, and periglacial landform classes summed with respect to physiographic region. Landform codes are as defined in Table 1. Physiographic region codes are defined in the methodology.

Of the 12 different mass movement landforms mapped, FL-SO accounts for ~56% of their combined area, with another ~33% from FL-DF. These two landforms are densest in OM physiographic unit, but FL-SO is common in EL and RM physiographic unis, and FL-DF in KP and EL. Also notable are FL-RTS that are concentrated at PPT.

Periglacial landforms are negligible at KP and TT but are otherwise common. Ice wedge polygons are the densest landforms, and ~51% of periglacial landform area is dominated by the thermokarst phase (IWP-H), but the active growth phase (IWP-L) is common at TC (23 km^2; ~10% of periglacial landform area). Nearly 26% of periglacial landform area is PEATP that is most dense in PPL (5.1%) and AP (1.8%) and with notable densities in MD (0.8%) and EL (0.5%). Finally, SNF are also commonplace, but are concentrated in PPL (1.3%), AP (0.8%), TC (0.4), and OM (0.2%).

4 Discussion

Our summary of landforms mapped within the DH-ITH corridor has demonstrated that the spatial distributions of the hydrological, mass movement, and periglacial landforms in the vicinity of the DH-ITH vary according to permafrost extent and ground ice condition, surficial geology, glacial history, and physiographic region (Table 1; Figures 1 and 3 to 5). Periglacial and hydrological features are concentrated in the northern portion of the corridor and coincide with terrains that were glaciated and have continuous permafrost with medium-high and high ground ice content, whereas mass movement features dominate the southern portion of the corridor, most of which was unglaciated during the Wisconsinan.

Hydrological landforms are most densely distributed throughout GLA terrain (~93% of hydrological landform area), with continuous permafrost and high ground ice contents (CH) (~92% of hydrological landform area), and with relatively low relief terrains associated with glacial deposits (GF, GL, M), Holocene thermokarst lake basins (L), and alluvium (A) and organic (O) deposits. The combinations of these conditions promote dense distributions of hydrological landforms in PPL, AP, MD, and TC physiographic units, which are dominated by TL landforms though DLB-P are common in PPL and TC. Hydrological landforms are sparse within UGLA terrain, with BS being most dense. Together these findings emphasize the influence that ice-rich glacial deposits have had on both past and contemporary thermokarst development, and likely on future thermokarst associated with climate warming.

Mass movement landforms, in contrast to hydrological landforms, are densest and most extensive in UGLA (~86% of mass movement landform area), where there is low and low-to-medium ground ice content in permafrost (~90% of mass movement area), and especially where there is C surficial geology unit (~66% mass movement area). Consequently, this class of landforms is extensive within OM, EL, RM physiographic units (~94% mass movement area) that have high relative relief. FL-SO and FL-DF landforms dominate this landform class. Locally common, FL-RG occurs exclusively within OM (~3% of mass movement landform area), and within GLA, FL-RTS (~3% mass movement area) have densities ≥0.1% in RM, PPT, and TC physiographic units. These findings demonstrate the influence that location with respect to the Laurentide Ice Sheet margin has on the spatial variation of mass movement landforms. They further suggest and that FL-SO, FL-DF, and FL-RG likely deserve more scientific attention, which in northwestern Canada has predominantly focused on FL-RTS (e.g., Kokelj et al. 2017, 2021).

Periglacial landforms are the most numerous, extensive, and densest landform class, occurring throughout the corridor region within GLA and UGLA, all permafrost units, and nearly all surficial geology units. However, they are concentrated in continuous permafrost of GLA, where there are glacial or modified glacial surficial deposits (M, GF, GL, and L). Though nearly 25% of O comprises mappable periglacial landforms, as with GL and E it comprises <1% of the corridor area. In high-relief, UGLA terrain the most densely distributed landform is IWP-H (OM, EL, RM physiographic units) as frost cracking was likely promoted throughout the Wisconsinan in C and A surficial geology units, whereas permafrost was obliterated beneath the Laurentide Ice Sheet in many places that were glaciated (Rampton 1988). The thermokarst phase (IWP-H) is dominant everywhere ice wedges were mapped, including

TC physiographic unit, where there is a notable density of IWP-L (2.5%) and many ice wedges in TC are known to be active (e.g., Kokelj et al. 2014). Within PPL and AP physiographic units, PEATP and SNF are comparatively dense, where we have observed that the gently sloping, rolling terrain has widespread areas of poor drainage that have promoted extensive permafrost peatlands and wetlands. Pingos, although of cultural and scientific interest, have a density of only 0.1% in TC where they are among the most concentrated in the world (Mackay 1963; Wolfe et al. 2023), but contribute little to the regional density of periglacial landforms.

Primarily a desktop study, the main database limitation is the CDEM used for 3-D visualization. It was available for the entire study area, but its ~20-m resolution is not well matched to the satellite imagery. This created some difficulty identifying and/or delineating some landforms. In such cases, available high-resolution LiDAR data were consulted. Other limitations relate to using optical imagery and the ground being obscured in places by cloud cover or shadow, or temporal or spatial breaks between satellite images that may have influenced identification of some features. Finally, some digitized landforms may have offset geographic positions due to the difficulty of orthorectifying satellite imagery in some areas due to insufficient ground control points. Human errors during landform mapping likely exist but were minimized using standardized criteria and protocols to identify and digitize features, and landform digitization was evaluated in an iterative manner between two expert mappers (Sladen et al. 2021). We used the most appropriate attribute data available at the time of mapping, but these datasets are dated, and unit boundaries will likely change if they are refined in the future.

Our research sets the stage for future work including quantitative statistical analysis to improve understanding of how landforms combine and control environmental variables, and spatial analysis of specific periglacial landform types with respect to field-based observations of ground ice and with national-scale estimates of ice-wedge, segregated, and buried ground ice distributions (O'Neill et al. 2019). Our results can be used to train thaw susceptibility modelling for the entire corridor region following the machine learning approach of Rudy et al. (2019), complimenting available landform data. Further, specific landforms in the database may be compared to existing (e.g., Lantz et al. 2017) or developing (e.g., Kokelj et al. 2023) landform inventories to build a more robust understanding of controls on landform distributions and their fate in a changing climate, and to provide insights on methodological limitations and advantages of the various approaches. Finally, the mapping protocol has been modified and applied to develop an analogous landform database for a proposed transportation corridor that would link Yellowknife, NT, to Grays Bay, NU (Morse et al. 2023). Comparison of the two landscape transects (and potentially others) can facilitate improved understanding of permafrost landscape evolution in northern Canada. From a practical perspective, this analysis and data can be used to extend geohazard mapping such as that by McKillop et al. (2016) to the height of the land, which can inform decisions regarding highway realignments to address infrastructure integrity issues due to climate change (Stockton et al. (2021).

5 Conclusions

This is the first investigation to use a set of 25 permafrost-related landforms, derived from a comprehensive geodatabase, and demonstrate how their varying spatial distributions in northwestern Canada relate to differences in permafrost extent and ground ice conditions, surficial geology, and glacial history, which are characteristics inherent to regional physiographic variation. Using a multi-variate approach, the research shows the distribution of permafrost-related landforms and their combined influence on terrain sensitivity. This fine-scale mapping compliments other recent initiatives that advance a multivariate approach to understand landform combinations and drivers of variation in northwestern Canada (Kokelj at al. 2023).

Glacial history is a clear control on the distributions of hydrological and mass movement landform classes, in agreement with Kokelj et al. (2021). Hydrological landforms (predominantly TL) are most dense in northern glaciated terrains with rolling relief and relatively poor drainage, whereas mass movements (predominantly FL-SO and FL-DF) are concentrated in unglaciated terrain with high relative relief and comparatively good drainage. Periglacial landforms, dominated by IWP-H that occur throughout the corridor, have greatest densities in northern, glaciated terrains where 97% of FL-RTS area is mapped.

Permafrost exerts control on landform densities through its extent and ground ice content. Within extensive discontinuous permafrost terrain (southernmost ~100 km of the corridor), the density of permafrost-related landforms is low and comprises almost entirely mass movements FL-DF and SL-RS. Permafrost is continuous elsewhere, with higher landform densities in southern terrains where ice content is low-medium, and highest in northern terrains where ice content is high. Landform densities are low in permafrost with low to medium ice content, based on the generalized classification of Heginbottom et al. (1995).

Surficial geology units, which are influenced by landscape history and geological setting, have clear relationships to distributions of permafrost-related landforms. In mountainous, unglaciated terrains, landform densities are predominantly related to occurrences of C and A as these two units are extensive. In glaciated areas, M, A, GF, and L units are the most extensive (in descending order), but landforms are most dense in O, L, GL, GF, and M units (in descending order). Units with higher densities of permafrost-related landforms potentially have a higher climate response. Thus, based on surficial geology unit areas and landform densities, M, C, and A may represent the geological units with the most overall climate response as they account for 86% of total area and 71% of total landform area, especially M that accounts for > 30% of both land and landform areas.

Physiographic units reflect the terrain conditions they are characterized by and landform densities among them vary substantially. TC, located at the maximum extent of the Laurentide Ice Sheet, with extensive glacial deposits and ice-rich permafrost, has the highest density of landforms, which are dominantly periglacial and hydrological. Landform densities in PPL and MD are the same magnitude as TC, but MD is characterized by extensive TL hydrological landforms in A, whereas PPL has extensive PEATP and SNF in in contrast to extensive ice-wedge polygons within TC. From an area perspective, however, OM may exhibit the greatest physical response to climate change within this corridor even though permafrost generally has low to medium ice content. This is because OM has the second greatest area and the fourth highest density of landforms, which are predominantly FL-SO, FL-DF, and IWP-H that occur in association with C, A, and M deposits.

The suite of landform densities draws attention to types like solifluction, debris flows, and rock glaciers that are common and even locally widespread but have not received as much scientific attention as ice-wedge polygons or retrogressive thaw slumps.

6 Acknowledgements

This research was supported by Natural Resources Canada, Northwest Territories Geological Survey, and Transport Canada. The authors would like to highlight the significant contributions of Erik Duncan, Samuel Jardine, and Andrew Branson for meticulous identification and digitization of features. Marcus Phillips provided valuable feedback on the manuscript. Comments by anonymous reviewers are appreciated.

7 References

Bostock, H.S. 2014. 'Physiographic Regions of Canada', *Geological Survey of Canada* "A" Series Map 1254A, 3 sheets. doi:10.4095/293408.

Burn, C.R., Moore, J.L., O'Neill, H.B., Hayley, D.W., Trimble, J.R., Calmels, F., Orban, S.N., and Idrees, M. 2015. 'Permafrost Characterization of the Dempster Highway, Yukon and Northwest Territories', in *GeoQuébec 2015*, Proceedings of the 7th Canadian Permafrost Conference. Québec City, Québec, Canada: Paper 705.

Castagner, A. Brenning, A., Gruber, S., and Kokelj, S.V. 2023. 'Vertical Distribution of Excess Ice in Icy Sediments and its Statistical Estimation from Geotechnical Data (Tuktoyaktuk Coastlands and Anderson Plain, Northwest Territories)', *Arctic Science* 9(2), pp. 483–496. doi:10.1139/as-2021-0041.

Charbonneau, A.A. and Smith, D.J. 2018. 'An Inventory of Rock Glaciers in the Central British Columbia Coast Mountains, Canada, from High Resolution Google Earth Imagery', *Arctic, Antarctic, and Alpine Research* 50(1), e1489026. doi:10.1080/15230430.2018.14890.

Duk-Rodkin, A. and Hughes, O.L. 1992a. 'Surficial Geology, Fort McPherson-Bell River, Yukon-Northwest Territories', *Geological Survey of Canada* Map 1745A. doi:10.4095/184002.

Duk-Rodkin, A., and Hughes, O.L. 1992b. 'Surficial Geology, Arctic Red River, District Mackenzie, Northwest Territories', *Geological Survey of Canada* Map 1746A. doi:10.4095/184003.

Gibson, C., Cottenie, K., Gingras-Hill, T., Kokelj, S.V., Baltzer, J.L., Chasmer, L., and Turetsky, M.R., 2021. 'Mapping and Understanding the Vulnerability of Northern Peatlands to Permafrost Thaw at Scales Relevant to Community Adaptation Planning', *Environmental Research Letters* 16, 055022. doi:10.1088/1748-9326/abe74b.

Gordey, S.P. and Makepeace, A.J. 2003. 'Yukon Digital Geology (v.2)', *Geological Survey of Canada* Open File 1749. doi:10.4095/214639.

Heginbottom, J.A., Dubreuil, M.A., and Harker, P.T. 1995. 'Canada – Permafrost', in *National Atlas of Canada*, 5th edition. Natural Resources Canada, MCR 4177. doi:10.4095/294672.

Hjort, J., Streletskiy, D., Doré, G., Wu, Q., Bjella, K., and Luoto, M. 2022. 'Impacts of Permafrost Degradation on Infrastructure', *Nature Reviews Earth and Environment* 3, pp. 24–38. doi:10.1038/s43017-021-00247-8.

Kokelj, S.V. and Jorgenson, M.T. 2013. 'Advances in Thermokarst Research', *Permafrost and Periglacial Processes*, 24(2), pp. 108–119. doi:10.1002/ppp.1779.

Kokelj, S.V., Gingras-Hill, T., Daly, S.V., Morse, P.D., Wolfe, S.A., Rudy, A.C.A, et al. 2023. 'The Northwest Territories Thermokarst Mapping Collective: A Northern-Driven Mapping Collaborative Toward Understanding the Effects of Permafrost Thaw'. *Arctic Science* 9, pp. 886–918. doi:10.1139/AS-2023-0009.

Kokelj, S.V., Kokoszka, J., van der Sluijs, J., Rudy, A.C.A., Tunnicliffe, J., Shakil, S., Tank, S.E., and Zolkos, S. 2021. 'Thaw-driven Mass Wasting Couples Slopes with Downstream Systems, and Effects Propagate Through Arctic Drainage Networks', *The Cryosphere* 15, pp. 3059–3081. doi:10.5194/tc-15-3059-2021, 2021.

Kokelj, S.V., Tunnicliffe, J.F., and Lacelle, D. 2017. 'The Peel Plateau of Northwestern Canada: An ice-rich Hummocky Moraine Landscape in Transition', in O. Slaymaker(ed.), *Landscapes and Landforms of Western Canada*. Switzerland: Springer Cham, pp.109–122. Available at: https://doi.org/10.1007/978-3-319-44595-3_7.

Kokelj, S.V., Lantz, T.C., Wolfe, S.A., Kanigan, J.C., Morse, P.D., Coutts, R., Molina-Giraldo, N., and Burn, C.R. 2014. 'Distribution and Activity of Ice Wedges Across the Forest-tundra Transition, Western Arctic Canada', *Journal of Geophysical Research: Earth Surface* 119, pp. 2032–2047. doi:10.1002/2014JF003085.

Lantz, T., Steedman, A., Kokelj, S.V., and Segal, R. 2017. 'Inventory of Polygonal Terrain in the Tuktoyaktuk Coastlands, Northwest Territories', *Northwest Territories Geological Survey* NWT Open Report 2016-22. doi:10.46887/2016-022.

Luo, J., Niu, F., Lin, Z., Liu, M., Yin, G., and Gao, Z. 2022. 'Inventory and Frequency of Retrogressive Thaw Slumps in Permafrost Region of the Qinghai–Tibet Plateau', *Geophysical Research Letters* 49, e2022GL099829. doi:10.1029/2022GL099829.

Mackay, J.R. 1963. 'The Mackenzie Delta Area, N.W.T.', *Geographical Branch, Mines and Technical Surveys* Memoir 8.

Mathews, W.H. 1986. 'Physiographic Map of the Canadian Cordillera', *Geological Survey of Canada* "A" Series Map 1701A. doi:10.4095/122821.

McKillop, R.J., Brown, C.E., McParland, D.J., Sacco, D.A. and Coates, J. 2016. 'Inventory of Mass Movement Geohazards along the Dempster Highway, Yukon', *Yukon Geological Survey* Miscellaneous Report 17.

Morse, P.D., Parker, R.J.H., Smith, S.L., and Sladen, W.E. 2023. 'Permafrost-Related Landforms and Geotechnical Data Compilation, Yellowknife to Grays Bay Corridor Region, Slave Geological Province', *Geological Survey of Canada* Open File 8986. doi:10.4095/332017.

Natural Resources Canada (NRCan) 2023. 'Canada Digital Elevation Model, 1945-2011', *Government of Canada* Open Maps. Available at: https://open.canada.ca/data/en/dataset/7f245e4d-76c2-4caa-951a-45d1d2051333 [Accessed: 14 July 2023].

Northwest Territories Centre for Geomatics (NWTCG) 2020. 'Ecological Land Classification Photos, Spatial Data Warehouse (SDW)', *Northwest Territories Centre for Geomatics*, Government of Northwest Territories. Available at: https://www.maps.geomatics.gov.nt.ca/Html5Viewer/index.html?viewer=SDW [Accessed on 14 July, 2023].

Rampton, V.N. 1988. 'Quaternary Geology of Tuktoyaktuk Coastlands, Northwest Territories', *Geological Survey of Canada* Memoir 423. doi:10.4095/126937.

Roots, C. and Hart, C. 2004. 'Bedrock Geology', in C.A.S. Smith, J.C. Meikle and C.F. Roots (eds.), *Ecoregions of the Yukon Territory: Biophysical Properties of Yukon Landscapes*. Summerland, British Columbia, Canada: Agriculture and Agri-Food Canada, pp. 11–14.

Rudy, A.C.A., Morse, P.D., Kokelj, S.V., Sladen, W.E., and Smith, S.L. 2019. 'A New Protocol to Map Permafrost Geomorphic Features and Advance Thaw-Susceptibility Modelling', in J.-P. Bilodeau, D.F. Nadeau, D. Fortier and D. Conciatori (eds.) *Cold Regions Engineering 2019*, proceedings of the 18th International Conference on Cold Regions Engineering and the 8th Canadian Permafrost Conference. Québec City, Québec, Canada: pp. 661–669. doi:10.1061/9780784482599.

Sladen, W.E., Parker, R.J.H., Kokelj, S.V., and Morse, P.D. 2021. 'Geomorphologic Feature Mapping Methodology Developed for the Dempster Highway and Inuvik to Tuktoyaktuk Highway Corridors', *Geological Survey of Canada* Open File 8751. doi:10.4095/328181.

Sladen, W.E., Parker, R.J.H., Morse, P.D., Kokelj, S.V., and Smith, S.L. 2022. 'Geomorphic Feature Inventory Along the Dempster and Inuvik to Tuktoyaktuk Highway Corridor, Yukon and Northwest Territories', *Geological Survey of Canada* Open File 8885. doi:10.4095/329969.

Stockton, E.J., Burn, C.R., and Humphries, J. (eds.) 2021. 'Compendium of Permafrost Reports: Northern Transportation Adaptation Initiative (NTAI) 2011-2021', *Carleton University*, Ottawa, Ontario. doi:10.52381/CPR.NTAI.2021.

Thomas, R.D. and Rampton, V.N. 1982a. 'Surficial Geology and Geomorphology North Klondike River, Yukon Territory', *Geological Survey of Canada* Preliminary Map 6-1982. doi:10.4095/119397.

Thomas, R.D. and Rampton, V.N. 1982b. 'Surficial Geology and Geomorphology Upper Blackstone River, Yukon Territory', *Geological Survey of Canada* Preliminary Map 7-1982. doi:10.4095/119066.

Thomas, R.D. and Rampton, V.N. 1982c. Surficial Geology and Geomorphology Engineer Creek, Yukon Territory, Preliminary Map 8-1982, Geological Survey of Canada, Ottawa, ON, Canada. doi:10.4095/119068.

Thomas, R.D. and Rampton, V.N. 1982d. 'Surficial Geology and Geomorphology Lower Ogilvie River, Yukon Territory', *Geological Survey of Canada* Preliminary Map 9-1982. doi:10.4095/119382.

Thomas, R.D. and Rampton, V.N. 1982e. 'Surficial Geology and Geomorphology Moose Lake, Yukon Territory', *Geological Survey of Canada* Preliminary Map 10-1982. doi:10.4095/119383.

Thomas, R.D. and Rampton, V.N. 1982f. 'Surficial Geology and Geomorphology Rock River, Yukon Territory', *Geological Survey of Canada* Preliminary Map 11-1982. doi:10.4095/119386.

Weiss, N., Kokelj, S.V., Rudy, A.C.A., Baltzer, J.L., Daly, S.V., Ferguson, C., Gingras-Hill, T., Morse, P.D., Paul, J.R., Pope, M., Wilson, A., and Wolfe, S.A. 2021. 'Contrasts in NWT Community Sensitivity to Permafrost Thaw from Broad-Scale Thermokarst Mapping', *Northwest Territories Geological Survey*. Available at: https://www.nwtgeoscience.ca/gsforum/contrasts-nwt-community-sensitivity-permafrost-thaw-broad-scale-thermokarst-mapping.

Wolfe, S.A, Morse, P.D., Parker, R., and Philips, M. 2023. 'Distribution and Morphometry of Pingos, Western Canadian Arctic, Northwest Territories, Canada', *Geomorphology* 431, 108694. doi:10.1016/j.geomorph.2023.108694.